


Metabolic Syndrome Predisposes to Osteoarthritis: Lessons from Model System

CARTILAGE
2021, Vol. 13(Suppl 1) 1598S–1609S
© The Author(s) 2020
Article reuse guidelines:
sagepub.com/journals-permissions
DOI: 10.1177/1947603520980161
journals.sagepub.com/home/CAR


Sampath Samuel Joshua Pragasam¹ 
and Vijayalakshmi Venkatesan¹ 

Abstract

Objective. The present study aims to assess for temporal changes in tibial subchondral bone and cartilage in WNIN/Gr-Ob rats (portraying obesity, insulin resistance, dyslipidemia, impaired glucose tolerance, hypertension) in comparison with Wistar controls (WNIN) using anthropometry, micro-computed tomography (micro-CT), scanning electron microscopy (SEM), histopathology, enzyme-linked immunosorbent assay (ELISA), and immunofluorescence. **Design.** Body weight, abdominal circumference, body mass index (BMI), lean/fat mass, serum tumor necrosis factor (TNF)- α levels were measured (ELISA), followed by ultrastructural analysis of tibial subchondral bone (micro-CT) and cartilage architecture (histopathology and SEM) in WNIN/Gr-Ob and WNIN rats with age (3, 6 and 9 months). Additionally, primary cultures of articular chondrocytes isolated from 6-month-old WNIN/Gr-Ob and WNIN rats were assessed for matrix metalloproteinase (MMP)-13 and Collagen type II (COL2A1) by immunofluorescence. **Results.** WNIN/Gr-Ob rats exhibited frank obesity with increased BMI, lean and fat mass vis-à-vis significantly higher levels of serum TNF- α (6>9>3 months) as compared with the controls. With an increase in BMI, WNIN/Gr-Ob rats presented with tibial cartilage fibrillation, erosion, osteophyte formation (6 months) and subchondral bone cyst (9 months) confirmed by histology and SEM. An increase in subchondral trabecular bone volume (sclerosis with decreased plate porosity) was observed in all ages in WNIN/Gr-Ob rats compared to their Control. Gaining insights, primary cultures of articular chondrocytes complemented with altered cellular expressions of COL2A1 and MMP-13 from WNIN/Gr-Ob rats, indicating osteoarthritis (OA) progression. **Conclusion.** Multiple metabolic perturbations featured in WNIN/Gr-Ob rats were effective to induce spontaneous OA-like degenerative changes affecting knee joints akin to human OA.

Keywords

osteoarthritis, WNIN/Gr-Ob, obesity, metabolic syndrome, knee joints, chondrocytes

Introduction

Traditionally, osteoarthritis (OA) has been considered to be a “wear and tear” disease leading to loss of articular cartilage. But this paradigm has been profoundly challenged owing to advances in epidemiology and basic research in OA.¹ No longer conceived as a simplex disease, OA has now been established as a disease of the whole joint, characterized by articular cartilage degeneration, subchondral bone remodeling, osteophyte formation, and synovial inflammation. Multiple risk factors, including age, gender, family history, obesity, occupation, injury, and joint morphology have been attributed to OA leading to the identification of many phenotypes like post-traumatic, aging-related, genetic, and symptomatic OA.²

Of late, the interlink between metabolic disorders and OA has been a subject of tremendous interest. Metabolic syndrome (MetS) also known as the “deadly quartet syndrome”

is a constellation that includes glucose intolerance (diabetes/ impaired glucose tolerance [IGT]), insulin resistance (IR), central obesity, and dyslipidemia—all well-documented risk factors for cardiovascular diseases.³ Evidence(s) from epidemiological and clinical studies strongly advocate for a role of MetS in the incidence and progression of OA, thereby proposing the concept of metabolic OA.⁴ Recent studies have demonstrated that MetS featured by dyslipidemia,

¹Stem Cell Research Laboratory, Department of Cell and Molecular Biology, National Institute of Nutrition (Indian Council of Medical Research), Tarnaka, Hyderabad, Telangana, India

Corresponding Author:

Vijayalakshmi Venkatesan, Stem Cell Research Division, Department of Cell and Molecular Biology, National Institute of Nutrition (Indian Council of Medical Research), Jamai Osmania (P.O.), Hyderabad, Telangana, 500007, India.
Email: v.venkateshan@gmail.com

insulin resistance, hypertension, adipokines derived from adipose tissues and low-grade inflammation could deregulate metabolism of the joint leading to OA.⁵ In similar lines, a recent report on several prospective cohorts showed that obese patients with MetS had an increased risk of incidence and severity of knee and hand OA⁶ and with an increase in each of the components of MetS, the risk of acquiring OA rose significantly.⁷ Very recently, Courties *et al.*⁸ had extensively reviewed the phenotypic approach to MetS-associated OA, underscoring the importance of obesity, MetS, and low-grade inflammation in OA pathogenesis.

Animal models are critical research tools in studying disease pathogenesis and drug discovery programs.⁹ With few *in vivo* model systems currently available for MetS-associated OA, it necessitates for identification of newer animal models to study metabolic OA. WNIN/Gr-Ob rat strain is a new entrant of obese animal models derived indigenously from the inbred Wistar rat (WNIN) colony of our institute maintained since 1920. The WNIN/Gr-Ob strain exhibits three distinct phenotypes consisting of homozygous lean (+/+), heterozygous carrier (+/-), and homozygous obese (-/-), following the Mendelian ratio of 1:2:1 inherited by autosomal incomplete dominance.¹⁰ From 35 days of age, these mutants portray noticeable spontaneous obesity and a kinky tail.¹¹ With age, an exponential increase in body weight accompanied by hyperphagia, polydipsia, polyuria, and glycosuria are observed in these rats.¹² They also portray altered biochemical and metabolic features like IR, IGT, hyperinsulinemia, hypertriglyceridemia, hypercholesterolemia, hyperleptinaemia, and hypertension^{11,12} with hypertrophy of the insulin-sensitive target organs. They depict accelerated aging with a shortened life span of 1.5 years and display an array of secondary complications warranting their application(s) in biomedical research, more pertinent to the area of MetS.¹³ Earlier studies have identified WNIN/Gr-Ob mutant rats to exhibit MetS^{14,15} and associated complications such as pancreatitis,¹⁶ retinal degeneration,¹³ and cataract.¹⁷

Therefore, we hypothesize that the WNIN/Gr-Ob rats portraying inherent MetS would serve as an optimal model to evaluate MetS-associated spontaneous OA-like changes (knee OA) akin to obese human subjects. We aim to investigate the WNIN/Gr-Ob rats for the presentation of spontaneous OA-like changes in their knee joints with increasing age vis-à-vis obesity (3, 6, and 9 months) compared with the age-matched WNIN controls.

Materials and Methods

Animals

All animal experiments were carried out in accordance with the guidelines of the Committee for the Purpose of Control

and Supervision of Experiments on Animals (CPCSEA). The study was reviewed and approved by the Institutional Animal Ethical Committee of the National Institute of Nutrition (NIN), Hyderabad (No. P29F/III-IAEC/NIN/12/2016). Inbred female WNIN/Gr-Ob obese littermates and control Wistar (WNIN) rats of varying ages (3, 6, and 9 months) were obtained from the Animal Facility, NIN and grouped according to their age. The rats were housed separately in standard polypropylene cages, maintained in temperature-controlled rooms at 22 ± 1 °C with 12-hour dark/light cycles and humidity of 50% to 60%. They were fed standard laboratory rat chow prepared at the animal facility with free access to water.

Anthropometrical Determinations

Body weight of the rats ($n = 6$ in each group) was measured using an electronic weight balance. The abdominal circumference and body length (nose-to-anus length) were also recorded. The BMI was calculated as $BMI = \text{bodyweight (g)} / \text{body length}^2 (\text{cm}^2)$.¹⁸

Body Composition Analysis Using EchoMRI

The body composition analysis to estimate fat mass and lean mass in the rats ($n = 6$ in each group) was carried out by magnetic resonance imaging¹⁹ using an EchoMRI (Echo Medical Systems, Houston, TX, USA) at Center for Cellular and Molecular Biology, Hyderabad.

Circulating Serum TNF- α Levels Using ELISA

The rats ($n = 6$ in each group) were fasted overnight, and blood was collected from the retro-orbital plexus into BD Vacutainer tubes. The serum was separated, and serum TNF- α was measured in duplicates using a commercially available ELISA kit (PeproTech, Cranbury, NJ, USA).

Micro-CT Assessment of Knee Joints

Post euthanasia by CO₂ asphyxiation, formalin-fixed knee joints of the rats ($n = 6$ in each group) were scanned and analyzed using SkyScan 1176 Micro-CT system and software (SkyScan, Kontich, Belgium) with voxel size 17.32 μm , voltage 50 kV, beam filtration filter 0.5 mm aluminum. After scanning, the knee joints were 3-dimensionally reconstructed by SkyScan ReCon software. For analyzing the subchondral plate, the load-bearing region with an area of $1.04 \times 1.04 \text{ mm}^2$ was selected as region of interest (ROI). Porosity of subchondral trabecular bone plate was measured and calculated using CT-Analyser software. For analysis of subchondral trabecular bone, a cuboid of trabecular bone with size of $1.04 \times 1.04 \times 0.52 \text{ mm}^3$ beneath the ROI of subchondral plate was selected. Percent bone volume

(BV/TV, %), trabecular thickness (TbTh, mm), trabecular separation (TbSp, mm), trabecular bone pattern factor (TbPf, 1/mm) were calculated for subchondral trabecular bone using CT-Analyser software.²⁰

Histopathological Examination

Tibiae of WNIN ($n = 6$) and WNIN/Gr-Ob rats ($n = 6$) at 3, 6, and 9 months were fixed in 10% neutral buffered formalin solution for 3 days and decalcified at 4 °C for 4 to 5 weeks with 0.5 M ethylenediaminetetraacetic acid (EDTA). The samples were dehydrated and embedded in paraffin by the standard method.²⁰ Serial sections of tibia were prepared in the sagittal plane at 5 to 7 μm and stained with hematoxylin and eosin (H&E). Images were captured using Nikon Eclipse TE2000-S Microscope (Japan). The Osteoarthritis Research Society International (OARSI) Scoring System was used to analyze the degenerative changes in the tibial cartilage²¹ and the samples were scored on a scale of 0 to 6, where 0= surface intact, cartilage morphology intact; 1= surface intact; 2= surface discontinuity; 3= vertical fissures (clefs); 4= erosion; 5= denudation; 6= deformation. The pathological changes in the subchondral bone were also graded between 0-4 according to the method of Aho *et al.*²² as follows: grade 0 = early stage of OA with no evident subchondral bone sclerosis, thin subchondral bone plate, and trabeculae. Articular cartilage is directly connected to bone marrow via open fenestrae (marked with an asterisk) in subchondral bone. Grade 1 = some subchondral sclerosis and bone volume is increased. Thickened bone trabeculae can be seen. Cartilage contact with bone marrow still persists. Grade 2 = a distinct increase in subchondral sclerosis and bone volume. Fibrillation can be seen in subchondral bone plate. No contact of bone marrow to articular cartilage can be identified. Grade 3 = late-stage disease. Severe subchondral sclerosis and massively increased bone volume. Bone marrow distance from cartilage increases. Subchondral bone plate flattens.

Ultrastructural Analysis of Tibial Cartilage Surface Using Scanning Electron Microscopy (SEM)

The tibiae were harvested from the rats ($n = 4$ in each group) and fixed overnight in Karnovsky's fixative. The fixed tissues were rinsed with distilled water, washed in phosphate buffered saline (PBS; 0.1 M, pH 7.2) and dehydrated in graded series of ethanol. Then the tissues were vacuum dried, mounted on aluminum stubs, sputter coated with gold, and scanned using Hitachi S-3400N scanning electron microscope.²³ The surface of the tibial cartilages was scanned and images were captured at various magnifications.

Isolation and Maintenance of Primary Articular Chondrocytes Cultures In Vitro

Primary articular chondrocytes were isolated from 6-month-old WNIN and WNIN/Gr-Ob rats as per the method of Oseni *et al.*²⁴ with slight modifications. Under sterile conditions, the femoral and tibial cartilage were collected, washed in PBS, digested in 0.15% collagenase-II for 4 hours at 37 °C, 5% CO₂, followed by addition of culture medium (Dulbecco's modified Eagle medium/Ham's F12 [1:1] supplemented with 10% fetal bovine serum, penicillin [100 IU/mL] and streptomycin [100 IU/mL]). The cell suspension was centrifuged at $300 \times g$ for 10 minutes, and the cell pellet was washed in culture medium and seeded in culture dishes, which were maintained at 37 °C, 5% CO₂ until confluency.

COL2A1 AND MMP-13 Expression in Primary Articular Chondrocytes Cultures by Immunofluorescence

For immunofluorescence studies, the chondrocytes (P1) grown on coverslips were fixed in 4% paraformaldehyde, washed with PBS, permeabilized with 50% chilled methanol, serum-blocked with 4% horse serum and incubated overnight at 4 °C with primary antibodies specific to COL2A1 (1:25; Developmental Studies Hybridoma Bank) and MMP-13 (1:100; Abcam). The cells were washed with PBS, incubated with a Cy-3-labeled secondary antibody (1:200 dilution) (Jackson Laboratories, USA) for 1 hour at room temperature, washed with PBS and mounted using DAPI (Vectashield, Vector Laboratories, USA). All images were captured using Leica Advanced Fluorescence software in a Leica TCS SP5 Confocal Microscope (Mannheim, Germany). The fluorescence intensities were calculated as relative fluorescent units (RFU) using the LAF software and represented as RFU per unit area.²⁵ Values are represented as mean \pm SD from 3 independent experiments performed in duplicate.

Statistical Analysis

Statistical analysis was carried out using SPSS Statistics software V.21. Comparison between WNIN and WNIN/Gr-Ob rats were made using Wilcoxon test. A P value < 0.05 was considered to be significant. For comparison of ultrastructure properties among the medial and lateral sides of WNIN/Gr-Ob and WNIN rats, *post hoc* multiple comparisons between groups were made using the Kruskal-Wallis test. If the Kruskal-Wallis test result was significant ($P < 0.05$), pairwise comparisons using a Wilcoxon test with Bonferroni correction to correct for multiple comparisons was made.

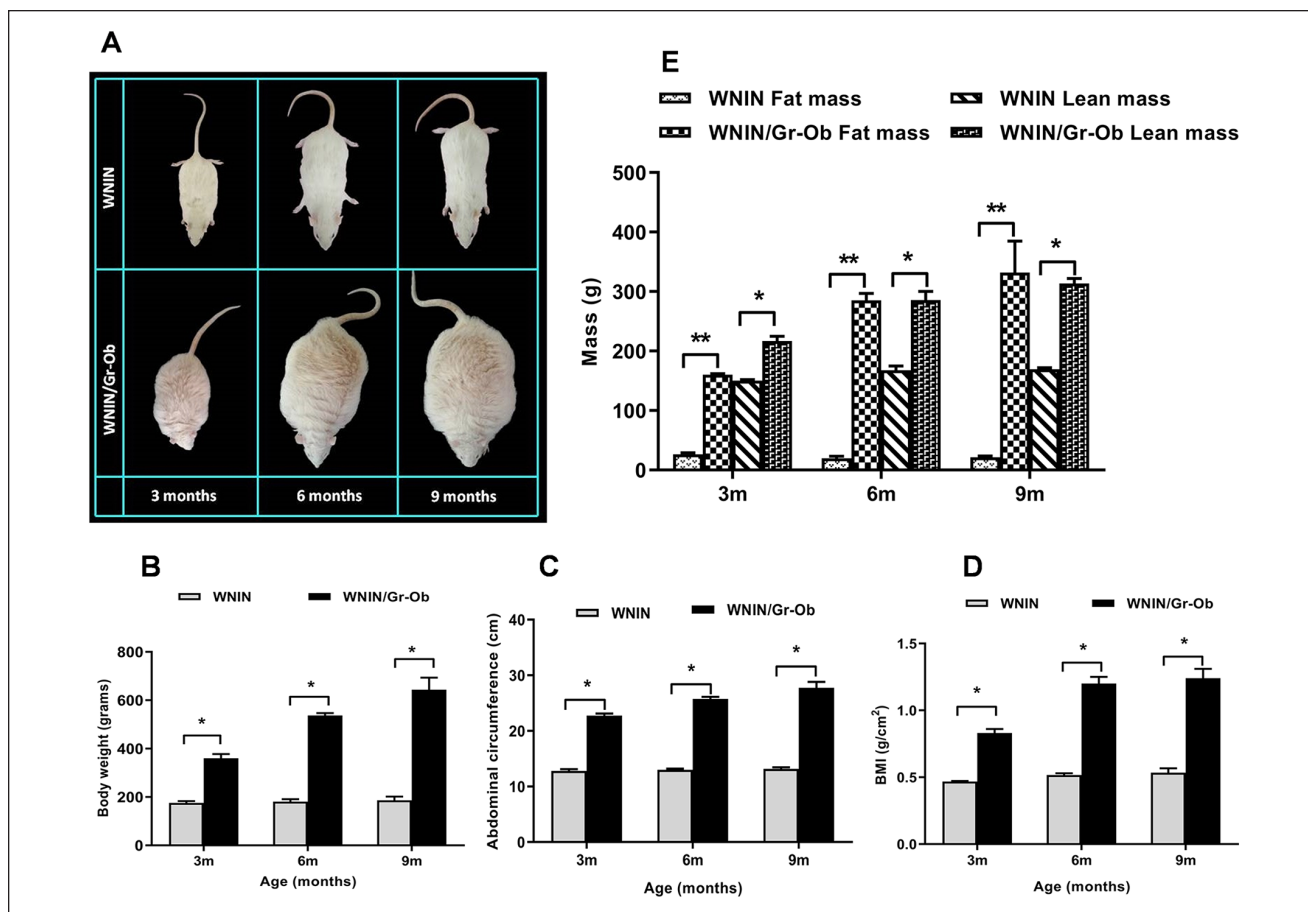


Figure 1. Anthropometric and body composition measurements (A) Representative photographic images of WNIN and WNIN/Gr-Ob rats at 3, 6, and 9 months of age. (B) Body weight, (C) abdominal circumference, (D) body mass index (BMI), and (E) lean mass and fat mass measurements in WNIN and WNIN/Gr-Ob rats at 3, 6, and 9 months of age. Values are expressed as mean \pm SD ($n = 6$). * $P < 0.05$; ** $P < 0.01$. Comparisons were made against age-matched WNIN controls.

Results

Increase in Body Weight, Abdominal Circumference, and BMI in WNIN/Gr-Ob Rats with Increase in Age

With increase in age, there was a significant increase in body weight (Fig. 1B) ($P < 0.05$), abdominal circumference (Fig. 1C) ($P < 0.05$), and BMI (Fig. 1D) ($P < 0.01$) in WNIN/Gr-Ob rats compared with the age-matched WNIN control rats, indicative of an increase in central obesity with age—a key risk factor predisposing for OA.

Higher Fat Mass and Lean Mass in WNIN/Gr-Ob Mutant Rats

There was a significant increase in both fat mass ($P < 0.01$) and lean mass ($P < 0.05$) (Fig. 1E) in WNIN/Gr-Ob mutant rats when compared to the WNIN rats with increase in age. Increase in fat composition not only adds up to the body

weight but also serves as “fat depots” acting as a source of cytokines and adipokines leading to a generalized inflammatory status of the animals.

Increased Circulating Levels of Pro-Inflammatory Cytokine TNF- α in WNIN/Gr-Ob Rats

There was a significant increase in TNF- α level in WNIN/Gr-Ob rats compared with WNIN rats at 6 and 9 months of age, with the highest levels at 6 months of age (Fig. 2) ($P < 0.05$). This is indicative of low-grade systemic inflammation in WNIN/Gr-Ob rats, which is a potential risk factor for the initiation and progression of osteoarthritis.

Subchondral Bone Plate: Lower Porosity in WNIN/Gr-Ob Mutant Rats

The ROI selection for subchondral bone plate is shown in Fig. 3A. Medial subchondral bone plate porosity was significantly lower in WNIN/Gr-Ob rats compared to WNIN

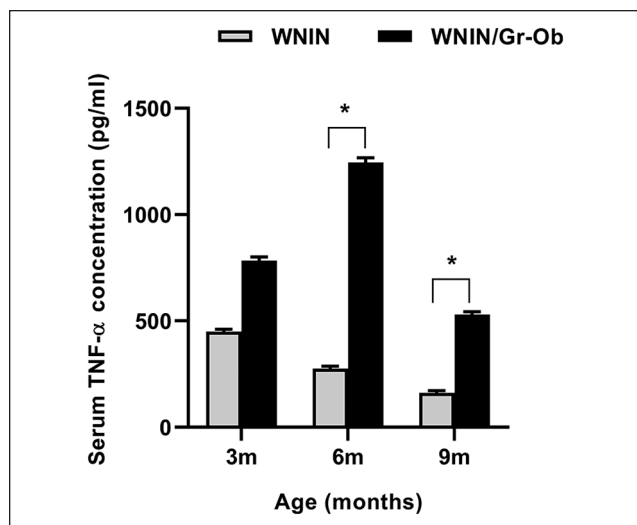


Figure 2. Quantitative analysis of serum tumor necrosis factor (TNF)- α by enzyme-linked immunosorbent assay (ELISA). Values are expressed as mean \pm SD ($n = 6$). * $P < 0.05$. Comparisons were made against age-matched WNIN controls.

rats at 6 and 9 months (**Fig. 3B**) ($P < 0.01$). Furthermore, in WNIN/Gr-Ob rats, the porosity of medial subchondral plate was significantly lower when compared with the lateral subchondral bone plate ($P < 0.05$). In WNIN group, decrease in subchondral bone plate porosity was 19% in medial side at 9 months compared with 3 months, whereas in the WNIN/Gr-Ob group, the decrease was 97%.

Subchondral Trabecular Bone: Higher BV/TV in WNIN/Gr-Ob Rats

The ROI selection of medial and lateral tibial subchondral trabecular bone is shown in **Fig. 3C**. Reconstructed cross-sections through the femur and tibia of WNIN and WNIN/Gr-Ob rats are shown in **Fig. 3D**. In WNIN/Gr-Ob rats, a significant reduction in porosity and increased bone formation was observed in the subchondral trabecular bone (**▶**) compared with WNIN rats at 6 and 9 months of age. This could possibly be attributed to increased bone formation through osteoblast differentiation. The results of micro-CT analysis on 3D ultrastructure parameters of subchondral trabecular bone of WNIN and WNIN/Gr-Ob rats are summarized in **Table 1**.

BV/TV was significantly higher ($P < 0.05$) in medial as well as lateral subchondral trabecular bone of WNIN/Gr-Ob group at 3, 6, and 9 months compared with WNIN group. Within the WNIN/Gr-Ob group, BV/TV was significantly higher ($P < 0.05$) in medial side than lateral side at 3, 6, and 9 months. TbTh was significantly greater ($P < 0.05$) in WNIN/Gr-Ob group than in the WNIN group in all 3 age groups. TbTh increased in WNIN/Gr-Ob strain at age of 6

and 9 months in medial side and decreased at 9 months in the lateral sides. In WNIN strain, TbTh increased in lateral side at 6 months. TbSp was significantly lower ($P < 0.05$) in WNIN/Gr-Ob group compared with WNIN group at 6 and 9 months in the medial side and at 9 months in the lateral side. TbPf was significantly lower ($P < 0.05$) in WNIN/Gr-Ob group when compared to WNIN group in both medial and lateral sides at 6 and 9 months. Within WNIN/Gr-Ob group, TbPf significantly decreased in 6 months in medial and lateral sides compared to 3 months.

Histological Findings: Tibial Cartilage Erosion and Subchondral Sclerosis in WNIN/Gr-Ob Rats

Normal tissue architecture with no detectable abnormalities in both cartilage as well as subchondral bone was observed in WNIN rats at 3, 6, and 9 months (**Fig. 4A-C**). WNIN/Gr-Ob rats at 3 months of age revealed healthy cartilage (**Fig. 4D**) with a mild cleft (**Fig. 4G**). At 6 months, WNIN/Gr-Ob rats exhibited cartilage erosion, disorientation of chondron columns, cell death and cell clustering, subchondral sclerosis with bone thickening osteophyte formation (**Fig. 4E and H**) indicating onset and progression of OA. At 9 months, WNIN/Gr-Ob rats exhibited complete erosion of hyaline cartilage with deep clefts and fissures, complete disorganization with discontinuous tide mark and cell clustering, subchondral sclerosis and bone cyst indicating late-stage OA (**Fig. 4F and I**). The OARSI grading showed a significant increase in cartilage degeneration and erosion in WNIN/Gr-Ob rats at 6 and 9 months (**Fig. 4J**) (** $P < 0.01$). The subchondral bone grading also indicated a significant increase in sclerosis and bone thickening in WNIN/Gr-Ob rats at 6 and 9 months, indicating OA progression (**Fig. 4K**).

Scanning Electron Microscopy of Tibia: Cartilage Erosion in WNIN/Gr-Ob Mutant Rats with Increase in Age

WNIN rats exhibited a smooth cartilage surface with no abrasions or erosions across all 3 age groups (**Fig. 5A**). At 3 months, WNIN/Gr-Ob rats' cartilage surface exhibited a smooth contour presenting with intact superficial layer without breakage. At 6 months, the cartilage surface was rough with ulcerations and cracks (**Fig. 5B**). Erosion of cartilage surface with fibrillation and degeneration of collagen fibers into cilia was also observed. At 9 months, thinning of cartilage with severe erosion in the medial side was observed with disorientation and degeneration of collagenous fibers into thick bundles, exposing layers of underlying connective tissue (**Fig. 5B**). These degenerative changes observed at the tibial cartilage surface of WNIN/Gr-Ob rats showed the progression of OA with increase in age, mimicking human OA.

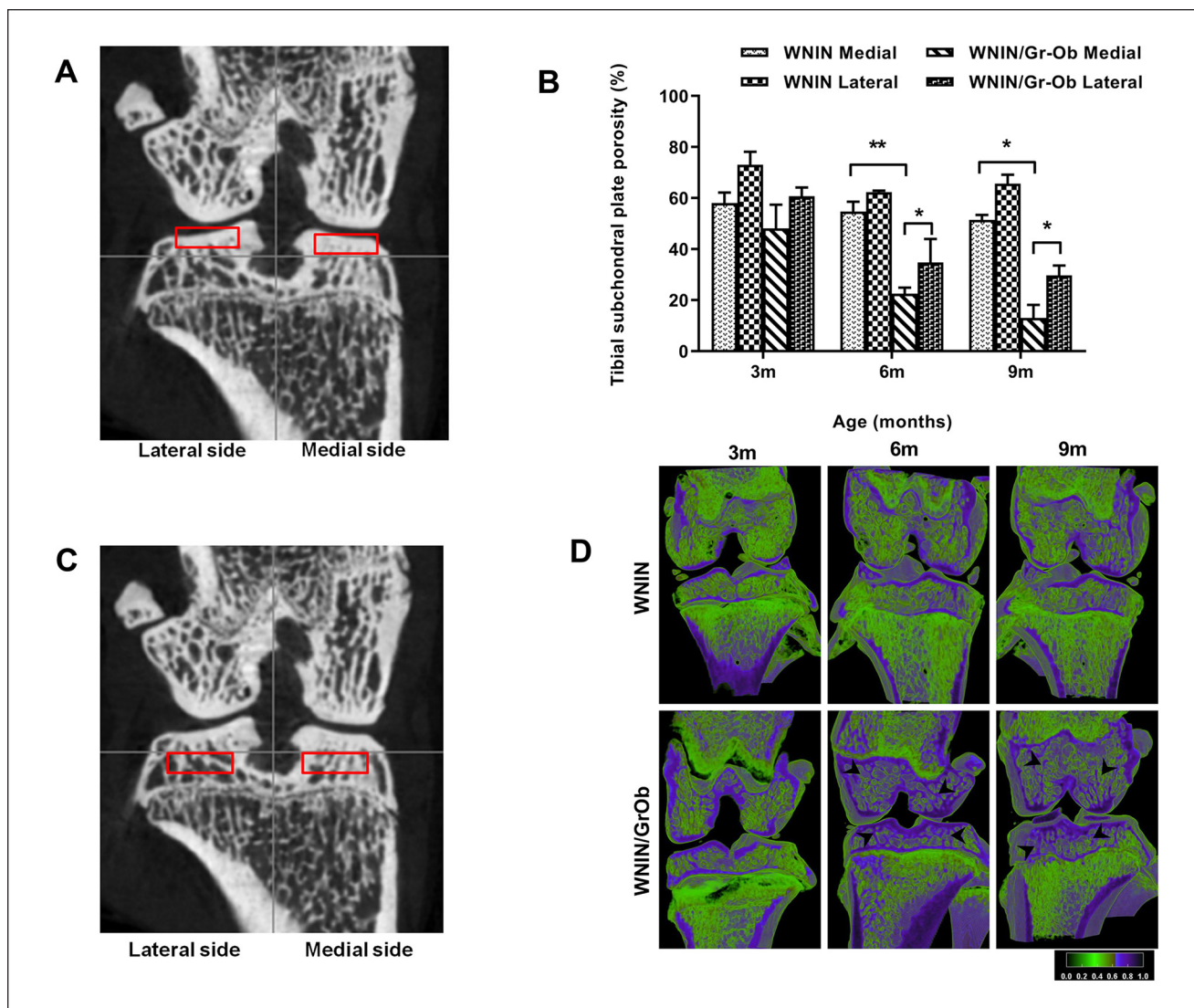


Figure 3. Micro-computed tomography (micro-CT) analysis of tibial subchondral plate and subchondral bone. **(A)** Demographic image of coronal view of region of interest (ROI) selection of medial and lateral tibial subchondral bone plate. **(B)** Quantitative analysis of subchondral plate porosity. **(C)** Demographic image of coronal view of ROI selection of medial and lateral tibial subchondral bone. **(D)** Reconstructed cross-sections through the intact knee joint (femur and tibia) showing significant reduction in bone porosity and increased bone formation (▶) in subchondral trabecular bone of WNIN/Gr-Ob rats compared with WNIN rats at 6 and 9 months of age. Values are expressed as mean \pm SD ($n = 6$). * $P < 0.05$; ** $P < 0.01$. Comparisons were made against age-matched WNIN controls.

Immunofluorescence Studies: Lower Expression of COL2A1 and Higher Expression of MMP-13 in WNIN/Gr-Ob Rats at 6 Months of Age

Taking inference from the previous experiments of this study, 6 months was chosen as an optimal age to assess the cellular expression of COL2A1 and MMP-13—the major catabolic effector in OA. WNIN/Gr-Ob rat chondrocytes expressed a significantly lower level of COL2A1 (Fig. 6A) ($P < 0.05$) and a significantly higher expression of MMP-13 (Fig. 6B) compared with WNIN articular chondrocytes

($P < 0.01$). These findings indicate onset of chondrocyte hypertrophy and initiation of OA at 6 months in WNIN/Gr-Ob rats.

Discussion

In the present study, we successfully demonstrate for the spontaneous onset and progression of knee OA in WNIN/Gr-Ob mutant obese rats which inherently portray biochemical and metabolic alterations, including obesity, dyslipidemia, IGT, IR, and hypertension. Articular cartilage degradation/

Table 1. Quantitative Micro-Computed Tomography Analysis of Subchondral Trabecular Bone (n = 6).

| | | WNIN-med | | WNIN-lat | | WNIN/Gr-Ob-med | | WNIN/Gr-Ob-lat | |
|--------------------|------|---------------------|--------|----------------------|--------|----------------------|--------|----------------------|--------|
| | | Mean | SD | Mean | SD | Mean | SD | Mean | SD |
| BV/TV (%) | 3 mo | 41.92 | 3.13 | 27.11 | 3.97 | 51.876 ^a | 4.882 | 39.28 ^a | 2.63 |
| | 6 mo | 45.33 [↑] | 2.99 | 34.36 [↑] | 2.73 | 77.45 ^{a↑} | 6.512 | 65.21 ^{a↑} | 2.92 |
| | 9 mo | 48.50 | 1.47 | 37.67 | 0.44 | 86.98 ^a | 3.966 | 70.26 ^a | 4.84 |
| TbTh (mm) | 3 mo | 0.1205 | 0.0035 | 0.1053 | 0.0054 | 0.1547 ^a | 0.0131 | 0.1337 ^a | 0.0014 |
| | 6 mo | 0.1388 | 0.0006 | 0.1374 [↑] | 0.0008 | 0.1888 ^{a↑} | 0.0316 | 0.1947 ^{a↑} | 0.0179 |
| | 9 mo | 0.1345 | 0.0006 | 0.1430 | 0.0068 | 0.1996 ^a | 0.0089 | 0.1791 ^a | 0.0002 |
| TbSp (mm) | 3 mo | 0.1758 | 0.0044 | 0.1999 | 0.0027 | 0.1737 | 0.0211 | 0.1921 | 0.0116 |
| | 6 mo | 0.1995 | 0.0129 | 0.1804 | 0.0086 | 0.1267 ^{b↓} | 0.0245 | 0.1615 | 0.0378 |
| | 9 mo | 0.1714 | 0.0067 | 0.2097 [↑] | 0.0025 | 0.1161 ^b | 0.0153 | 0.1591 ^b | 0.0053 |
| TbPf (1/mm) | 3 mo | 8.7198 | 0.3076 | 13.0045 | 0.5679 | 10.6395 | 0.1803 | 10.0843 | 0.7095 |
| | 6 mo | 7.1392 [↓] | 0.6094 | 10.4822 [↓] | 1.1138 | 2.6333 ^{b↓} | 0.8878 | 5.8246 ^{b↓} | 1.1668 |
| | 9 mo | 6.5485 | 0.2177 | 10.0233 | 0.1322 | 1.5598 ^b | 0.4384 | 4.6727 ^b | 1.1095 |

lat = lateral; med = medial; BV/TV = bone volume/total volume; TbTh = trabecular thickness; TbSp = trabecular separation; TbPf = trabecular bone pattern factor; [↑] = significant increase comparing with previous time point, P < 0.05; [↓] = significant decrease comparing with previous time point, P < 0.05.
^aSignificant increase compared with WNIN at the same time point, P < 0.05.
^bSignificant decrease compared with WNIN at the same time point, P < 0.05.

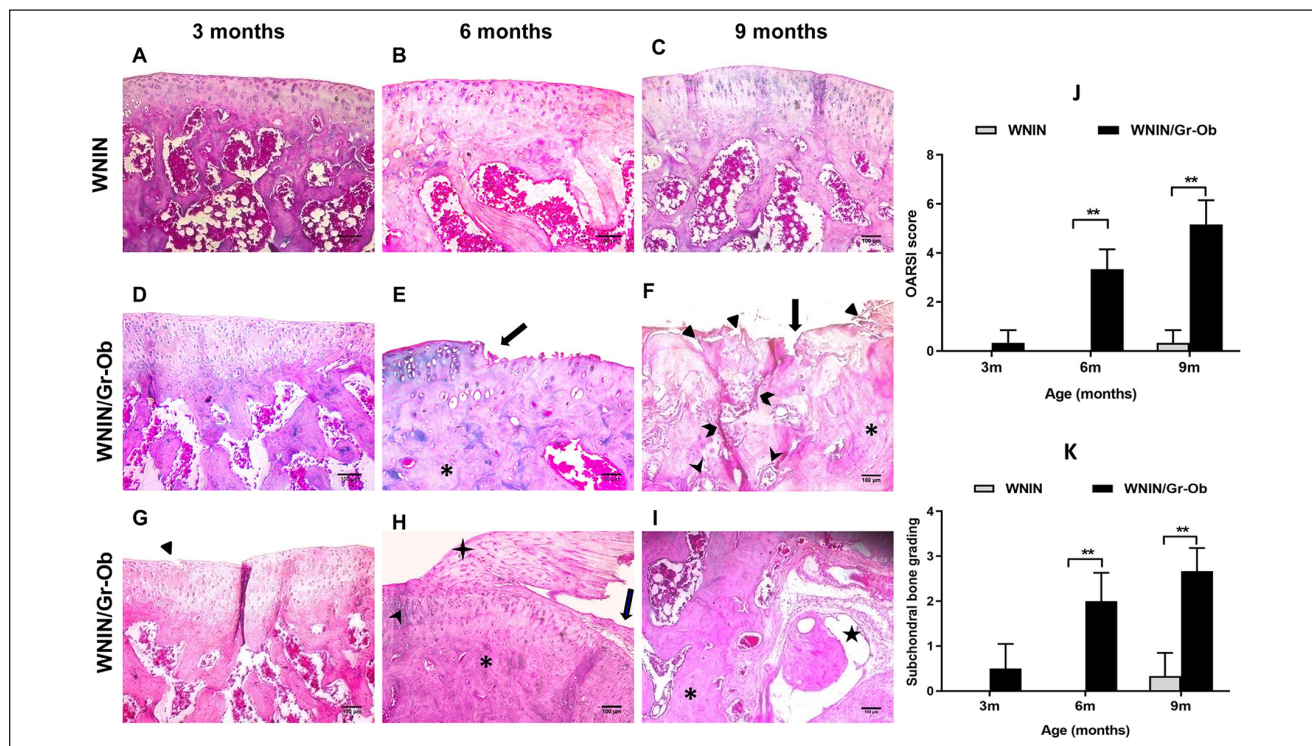


Figure 4. Histological analysis using hematoxylin and eosin (H&E) staining. (A-C) Normal full thickness cartilage and subchondral bone in WNIN rats at 3, 6, and 9 months (A, B, and C, respectively). (D) At 3 months, WNIN/Gr-Ob rats exhibited a healthy tibial cartilage (G) with a mild cleft (▲). (E) At 6 months of age, WNIN/Gr-Ob rats exhibited cartilage erosion (†) and a significant increase in subchondral sclerosis and bone volume (*) indicating onset and progression of osteoarthritis (OA). (H) At 6 months, WNIN/Gr-Ob rats also exhibited cartilage erosion (†), disorientation of chondron columns with cell death and cell clustering (▲), subchondral sclerosis, increase in bone volume (*) and osteophyte formation (+). (F) At 9 months of age, WNIN/Gr-Ob rats exhibited complete loss/erosion of hyaline cartilage with no chondrocytes (†) with deep clefts (▲) and vertical fissures (▶) extending into calcified cartilage, complete disorganization with discontinuous tide mark and cell clustering (▲), subchondral sclerosis and increase in bone volume (*) indicating late-stage OA. (I) Also, at 9 months, WNIN/Gr-Ob rats exhibited subchondral sclerosis (*) and bone cyst formation (★). (J) OARSI (Osteoarthritis Research Society International) scoring indicated that there was a significant cartilage degeneration indicating disease progression in WNIN/Gr-Ob rats at 6 and 9 months. (K) The subchondral sclerotic changes significantly increased in WNIN/Gr-Ob rats at 6 and 9 months. Values are expressed as Mean ± SD (n = 6). Comparisons were made with age-matched WNIN controls. **P < 0.01.

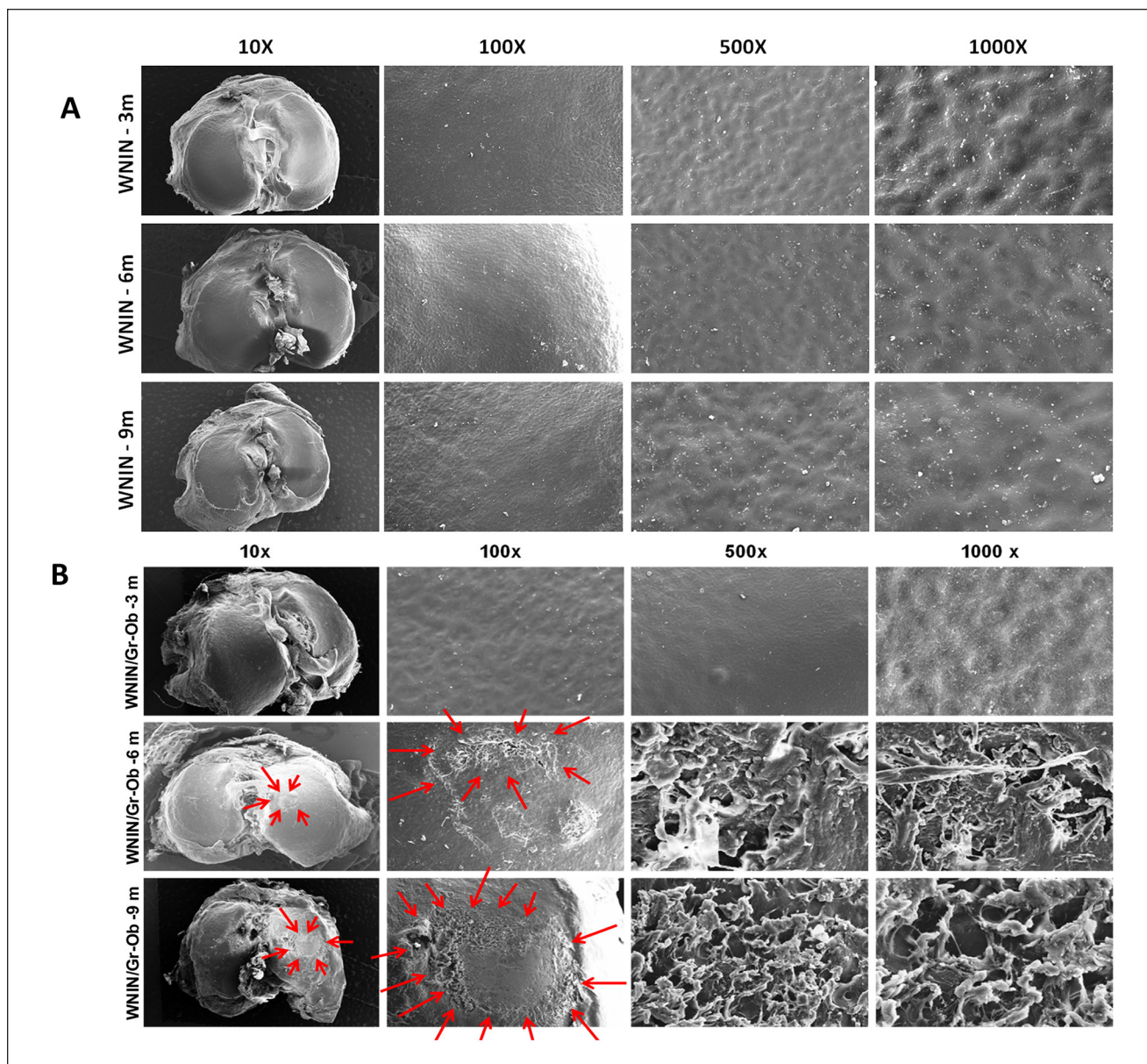


Figure 5. Scanning electron microscopy (SEM) assessment of tibial cartilage surface. **(A)** Representative SEM micrographs of WNIN rat tibial surfaces at 3, 6, and 9 months at different magnifications. **(B)** Representative SEM micrographs of WNIN/Gr-Ob rat tibial surfaces at 3, 6, and 9 months. The micrographs were captured at various magnifications (10 \times , 100 \times , 500 \times , and 1000 \times) ($n = 3$).

erosion with pathological alterations in subchondral bone in these WNIN/Gr-Ob rats (assessed by biochemical, micro-CT, histology and SEM analysis) accompanied by altered cellular expression of COL2A1 and MMP-13 in articular chondrocytes confirm the age-dependent progression of OA in the knee joints of these rats.

Obesity predominantly contributes to OA through increased loading on weight-bearing joints,²⁵ causing mechanical trauma in cartilage and bone. Human subjects with a BMI >30 kg/m² are 6.8 times more likely to develop knee OA than normal-weight controls.²⁶ Additionally,

obesity-related systemic factors vis-à-vis aberrantly expressed adipokines like leptin and cytokines like TNF- α stimulate the expression of MMPs and pro-inflammatory cytokines to exert direct and downstream detrimental effects on the cartilage, synovium, and bone leading to OA.²⁷ In our current study, the WNIN/Gr-Ob rats exhibited a significant increase in central obesity with age, as shown by increased bodyweight, abdominal circumference, BMI, fat mass, and lean mass. At 6 and 9 months, these rats exhibited abnormalities in tibial cartilage architecture such as thinning, fibrillation and severe erosion of cartilage with

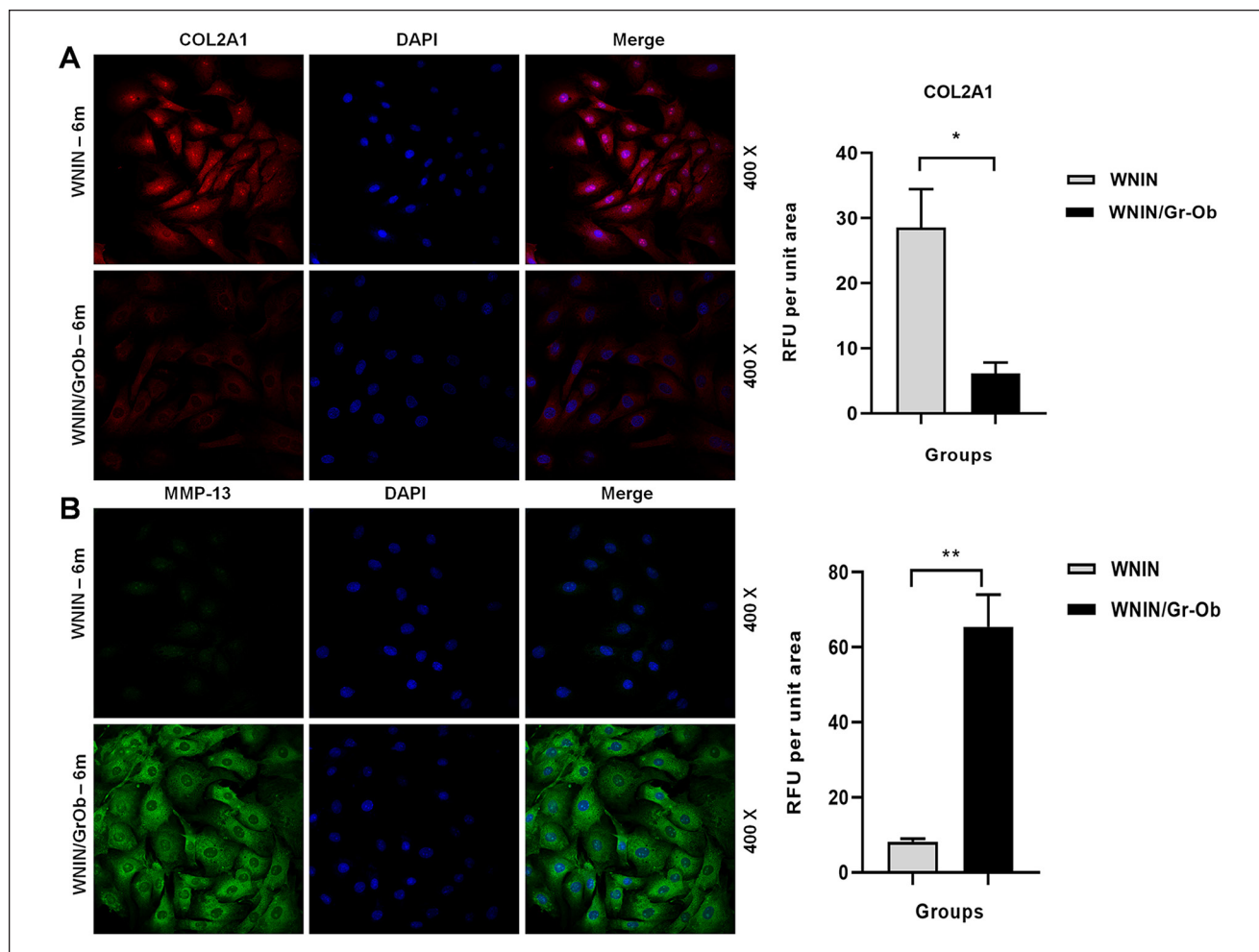


Figure 6. Immunofluorescence studies in primary articular chondrocytes of WNIN and WNIN/Gr-Ob rats at 6 months. **(A)** COL2A1 expression and **(B)** MMP-13 expression. The results represent 3 independent experiments. Values shown represented as mean \pm SD; * $P < 0.05$; ** $P < 0.01$. Comparisons were made against age-matched WNIN controls.

complete tissue disorganization, as evidenced by SEM and histology. With an increase in age, body weight, BMI, and fat mass content, the obesity-driven factors could be deemed guilty in inducing those above OA-associated degenerative changes of the tibiofemoral joints of these obese mutant rats.

Madhira *et al.*¹⁵ had earlier reported that these rats have an inherent obese phenotype memory in their bone marrow mesenchymal stem cells demonstrated by an upregulation of PPAR- γ (peroxisome proliferator-activated receptor gamma) expression and production of pro-inflammatory cytokines TNF- α and IL-6. In the present study, the circulating levels of TNF- α were found to be the highest in WNIN/Gr-Ob rats at 6 months, suggesting an optimal age for the initiation of OA-like changes in these rats. Using a high-fat diet mouse model of obesity/glucose intolerance and TNF-knockout, Hamada *et al.*²⁸ had demonstrated that IR and TNF- α -driven inflammation led to the initiation of OA in the mice thereby establishing a critical link between

metabolic dysfunction and OA initiation/progression. Our current findings in WNIN/Gr-Ob rats share a commonality with this reported evidence. We anticipate IR, obesity, and obesity-derived low-grade systemic inflammation could accelerate the initiation and progression of OA-like changes in these rats.

Subchondral bone alterations in OA patients and OA animal models have been well established. In the guinea pig model of spontaneous OA, subchondral sclerosis with trabecular ultrastructural turnover, lower porosity, and increased bone volume was observed in early-stage OA ahead of actual cartilage degeneration.²⁰ Subchondral sclerotic changes have also been reported in surgical^{29,30} and spontaneous rodent models of OA.³¹ In our study, we report for the first time subchondral bone sclerosis in WNIN/Gr-Ob obese rats, a model system already established in our laboratory to portray biochemical and metabolic perturbations akin to MetS. At 3 months, these rats exhibited subchondral sclerosis (micro-CT) with no identifiable articular cartilage

degeneration. At 6 and 9 months, the WNIN/Gr-Ob rats exhibited a significant increase in subchondral trabecular bone volume and a significant decrease in trabecular bone plate porosity accompanied by tibial cartilage degeneration. Expansion of the trabecular bone observed in subchondral bone undergoing excessive new bone formation reduces the size of the bone marrow spaces, potentially resulting in an ischemic state, or at the very least a change in tissue nutrition.³² The downstream nocent effects of subchondral ischemia include a compromised nutrient and gas exchange between the articular cartilage and bone, initiating degradative changes in the cartilage.³³ In our study, we believe that the subchondral sclerotic changes observed in WNIN/Gr-Ob rats could have possibly resulted in subchondral ischemia affecting the overlying cartilage both biologically and mechanically. Also, hypertension-induced vascular pathology could contribute to subchondral ischemia in these rats as they are inherently hypertensive. Other classic pathological features associated with OA, such as synovial inflammation, osteophyte formation, subchondral bone cyst, were also observed in these rats as revealed by histology. These novel findings add leverage to the plausible employability of WNIN/Gr-Ob mutant rats in OA research.

MMP-13 is a key proteinase holding a pivotal position in the cartilage degradation network and touted to be a potential biomarker for OA.³⁴ In clinical OA subjects³⁵ and in transgenic OA mice,³⁶ articular cartilage degradation was found to be associated with high MMP-13 expression, suggestive of its pathological role in OA. To gain deeper insights at the cellular level, articular chondrocytes were isolated from WNIN/Gr-Ob and WNIN rats at 6 months, the age at which key degenerative changes in cartilage began to manifest. Interestingly, immunofluorescence studies revealed significantly higher levels of MMP-13 (8.4-fold ↑) and lower levels of COL2A1 (4.6-fold ↓) in WNIN/Gr-Ob rats as compared with WNIN rats (6 months). COL2A1 is known to suppress articular chondrocyte hypertrophy, thereby preventing OA progression³⁷, while MMP-13 is a marker of hypertrophic chondrocytes in OA.³⁸ Our findings on COL2A1 and MMP-13 expression levels reveal the onset of chondrocyte hypertrophy (decrease in COL2A1) and initiation of early OA-like changes leading to cartilage degradation (increase in MMP-13) in the WNIN/Gr-Ob rats at 6 months alluding to the observations made by histopathology and ultrastructure analysis of cartilage.

Findings from the spontaneously hypersensitive heart failure (SHHF^{+/+}) rats,³⁹ Graham-Havel UC-Davis Type 2 Diabetes Mellitus (UCD-T2DM) rats,⁴⁰ high-fat diet-induced mice models have proven that metabolic disturbances/ altered metabolite signature accompanied by low-grade inflammation culminated in inducing spontaneous OA in these models. Hence it stands worthwhile to state that abnormal metabolic perturbations seen in WNIN/Gr-Ob rats could well precede the anatomic and physiological changes in joint tissue culmi-

nating in OA. In this context, this model may have its limitations in portraying other clinical phenotypes of OA.

In conclusion, we propose that the constellation of the metabolic alterations such as obesity, IR, hypertension, dyslipidemia, and inflammation exhibited by the WNIN/Gr-Ob rats aided by accelerated aging could coalesce to effect spontaneous OA-like changes (biochemical, histological, ultrastructural, and cellular) observed in their knee joints. These rats could provide a befitting model to evaluate the pathogenesis and pharmacotherapy of metabolic-OA en route the “natural progression” of the disease, without the need for any intervention to induce disease. Currently available rat models of osteoarthritis are either surgically/chemically induced models or genetically modified models and the number of spontaneously generating OA rat models are very scarce especially for the metabolic phenotype. In this context, our findings using the WNIN/Gr-Ob rats gain significance and novelty for their inherent ability to develop spontaneous OA aided by the assimilation of multiple metabolic risk factors.

Author Contributions

SSJP and VV have made substantial contributions to (1) the conception and design of the study, or acquisition of data, or analysis and interpretation of data; (2) drafting the article or revising it critically for important intellectual content; and (3) final approval of the version to be submitted.

Acknowledgments and Funding

The authors would like to thank Indian Council of Medical Research, New Delhi, for financial support to Sampath Samuel Joshua Pragasam through postdoctoral research fellowship (Postdoctoral Research Fellowship Grant No. 3/1/3/PDF (14)/2016-HRD), the Director of the institute for infrastructure support, Animal Facility, Mr. Madhusudhan Chary, Technical Officer for technical support in performing SEM.

Declaration of Conflicting Interests

The author(s) declared no potential conflicts of interest with respect to the research, authorship, and/or publication of this article.

Ethical Approval

All animal procedures were reviewed and approved by the Institutional Animal Ethical Committee, National Institute of Nutrition (NIN), Hyderabad (P29F/III-IAEC/NIN/12/2016). All the experiments were performed in accordance with the regulations and guidelines of the Committee for the Purpose of Control and Supervision of Experiments on Animals (CPCSEA).

ORCID iDs

Sampath Samuel Joshua Pragasam  <https://orcid.org/0000-0002-0789-8306>

Vijayalakshmi Venkatesan  <https://orcid.org/0000-0002-3142-9657>

References

- Courties A, Sellam J, Berenbaum F. Metabolic syndrome-associated osteoarthritis. *Curr Opin Rheumatol*. 2017;29(2):214-22.
- Wang X, Hunter D, Xu J, Ding C. Metabolic triggered inflammation in osteoarthritis. *Osteoarthritis Cartilage*. 2015;23(1):22-30.
- Oladejo AO. Overview of the metabolic syndrome; an emerging pandemic of public health significance. *Ann Ib Postgrad Med*. 2011;9(2):78-82.
- Shin D. Association between metabolic syndrome, radiographic knee osteoarthritis, and intensity of knee pain: results of a national survey. *J Clin Endocrinol Metab*. 2014;99:3177-83.
- Kluzek S, Newton JL, Arden NK. Is osteoarthritis a metabolic disorder? *Br Med Bull*. 2015;115:111-21.
- Berenbaum F. Osteoarthritis as an inflammatory disease (osteoarthritis is not osteoarthrosis!). *Osteoarthritis Cartilage*. 2013;21(1):16-21.
- Askari A, Ehrampoush E, Homayounfar R, Arasteh P, Naghizadeh MM, Yarahmadi M, *et al*. Relationship between metabolic syndrome and osteoarthritis: the Fasa Osteoarthritis Study. *Diabetes Metab Syndr*. 2017;11(Suppl 2):S827-S832.
- Courties A, Berenbaum F, Sellam J. The phenotypic approach to osteoarthritis: a look at metabolic syndrome-associated osteoarthritis. *Joint Bone Spine*. 2019;86(6):725-30.
- Little CB, Zaki S. What constitutes an “animal model of osteoarthritis”—the need for consensus? *Osteoarthritis Cartilage*. 2012;20(4):261-7.
- Singh H, Giridharan N, Bhonde R, Venkatesan V. Deriving at candidate genes of metabolic stress from pancreas of WNIN/GR-Ob mutant rats. *Islets*. 2013;5(4):133-8.
- Singh H, Ganneru S, Malakapalli V, Chalasani M, Nappanveetil G, Bhonde RR, Venkatesan V. Islet adaptation to obesity and insulin resistance in WNIN/GR-Ob rats. *Islets*. 2014;6(5-6):e998099.
- Harishankar N, Vajreswari A, Giridharan NV. WNIN/GR-Ob - an insulin-resistant obese rat model from inbred WNIN strain. *Indian J Med Res*. 2011;134(3):320-9.
- Godisela KK, Reddy SS, Kumar CU, Saravanan N, Reddy PY, Jablonski MM, *et al*. Impact of obesity with impaired glucose tolerance on retinal degeneration in a rat model of metabolic syndrome. *Mol Vis* 2017;23:263-74.
- Venkatesan V, Madhira SL, Malakapalli VM, Chalasani M, Shaik SN, Seshadri V, *et al*. Obesity, insulin resistance, and metabolic syndrome: a study in WNIN/Ob rats from a pancreatic perspective. *Biomed Res Int*. 2013;2013:617569.
- Madhira SL, Challa SS, Chalasani M, Nappanveethyl G, Bhonde RR, Ajumeera R, *et al*. Promise(s) of mesenchymal stem cells as an in vitro model system to depict pre-diabetic/diabetic milieu in WNIN/GR-Ob mutant rats. *PloS one*. 2012;7(10):e48061.
- Singh H, Ajumeera R, Malakapalli V, Chalasani M, Pothani S, Venkatesan V. WNIN mutant obese rats develop acute pancreatitis with the enhanced inflammatory milieu. *Cell Mol Med Res*. 2017;1:20-31.
- Reddy GB, Vasireddy V, Mandal MN, Tiruvalluru M, Wang XF, Jablonski MM, *et al*. A novel rat model with obesity-associated retinal degeneration. *Invest Ophthalmol Vis Sci*. 2009;50(7):3456-63.
- Novelli EL, Diniz YS, Galhardi CM, Ebaid GM, Rodrigues HG, Mani F, *et al*. Anthropometrical parameters and markers of obesity in rats. *Lab Anim*. 2007;41(1):111-9.
- Tinsley FC, Taicher GZ, Heiman ML. Evaluation of a quantitative magnetic resonance method for mouse whole body composition analysis. *Obes Res*. 2004;12(1):150-60.
- Wang T, Wen CY, Yan CH, Lu WW, Chiu KY. Spatial and temporal changes of subchondral bone proceed to microscopic articular cartilage degeneration in guinea pigs with spontaneous osteoarthritis. *Osteoarthritis Cartilage*. 2013;21(4):574-81.
- Pritzker KP, Gay S, Jimenez SA, Ostergaard K, Pelletier JP, Revell PA, *et al*. Osteoarthritis cartilage histopathology: grading and staging. *Osteoarthritis Cartilage*. 2006;14(1):13-29.
- Aho OM, Finnilä M, Thevenot J, Saarakkala S, Lehenkari P. Subchondral bone histology and grading in osteoarthritis. *PLoS One*. 2017;12(3):e0173726.
- Gomes A, Saha PP, Bhowmik T, Dasgupta AK, Dasgupta SC. Protection against osteoarthritis in experimental animals by nanogold conjugated snake venom protein toxin gold nanoparticle-Naja kaouthia cytotoxin 1. *Indian J Med Res*. 2016;144(6):910-7.
- Oseni AO, Butler PE, Seifalian AM. Optimization of chondrocyte isolation and characterization for large-scale cartilage tissue engineering. *J Surg Res*. 2013;181(1):41-8.
- Vincent HK, Heywood K, Connelly J, Hurley RW. Obesity and weight loss in the treatment and prevention of osteoarthritis. *PM R*. 2012;4(5 Suppl):S59-S67.
- Coggon D, Reading I, Croft P, McLaren M, Barrett D, Cooper C. Knee osteoarthritis and obesity. *Int J Obes Relat Metab Disord*. 2001;25(5):622-7.
- King LK, March L, Anandacoomarasamy A. Obesity & osteoarthritis. *Indian J Med Res*. 2013;138(2):185-93.
- Hamada D, Maynard R, Schott E, Drinkwater CJ, Ketz JP, Kates SL, *et al*. Suppressive effects of insulin on tumor necrosis factor-dependent early osteoarthritic changes associated with obesity and type 2 diabetes mellitus. *Arthritis Rheumatol*. 2016;68(6):1392-402.
- Fang H, Huang L, Welch I, Norley C, Holdsworth DW, Beier F, *et al*. Early changes of articular cartilage and subchondral bone in the DMM mouse model of osteoarthritis. *Sci Rep*. 2018;8(1):2855.
- Pickarski M, Hayami T, Zhuo Y, Duong LT. Molecular changes in articular cartilage and subchondral bone in the rat anterior cruciate ligament transection and meniscectomized models of osteoarthritis. *BMC Musculoskelet Disord*. 2011;12:197.
- Staines KA, Poulet B, Wentworth DN, Pitsillides AA. The STR/ort mouse model of spontaneous osteoarthritis—an update. *Osteoarthritis Cartilage*. 2017;25(6):802-8.
- Stewart HL, Kawcak CE. The importance of subchondral bone in the pathophysiology of osteoarthritis. *Front Vet Sci*. 2018;5:178.
- Zhuo Q, Yang W, Chen J, Wang Y. Metabolic syndrome meets osteoarthritis. *Nat Rev Rheumatol*. 2012;8(12):729-37.

34. Wang M, Sampson ER, Jin H, Li J, Ke QH, Im HJ, *et al.* MMP13 is a critical target gene during the progression of osteoarthritis. *Arthritis Res Ther.* 2013;15(1):R5.
35. Roach HI, Yamada N, Cheung KS, Tilley S, Clarke NM, Oreffo RO, *et al.* Association between the abnormal expression of matrix-degrading enzymes by human osteoarthritic chondrocytes and demethylation of specific CpG sites in the promoter regions. *Arthritis Rheum.* 2005;52(10):3110-24.
36. Neuhold LA, Killar L, Zhao W, Sung ML, Warner L, Kulik J, *et al.* Postnatal expression in hyaline cartilage of constitutively active human collagenase-3 (MMP-13) induces osteoarthritis in mice. *J Clin Invest.* 2001;107(1):35-44.
37. Lian C, Wang X, Qiu X, Wu Z, Gao B, Liu L, *et al.* Collagen type II suppresses articular chondrocyte hypertrophy and osteoarthritis progression by promoting integrin β 1-SMAD1 interaction. *Bone Res.* 2019;7:8.
38. van der Kraan PM, van den Berg WB. Chondrocyte hypertrophy and osteoarthritis: role in initiation and progression of cartilage degeneration? *Osteoarthritis Cartilage.* 2012;20(3):223-32.
39. Deng C, Bianchi A, Presle N, Moulin D, Koufany M, Guillaume C, *et al.* Eplerenone treatment alleviates the development of joint lesions in a new rat model of spontaneous metabolic-associated osteoarthritis. *Ann Rheum Dis.* 2018;77(2):315-6.
40. Onur T, Wu R, Metz L, Dang A. Characterisation of osteoarthritis in a small animal model of type 2 diabetes mellitus. *Bone & joint research.* 2014;3(6):203-211.